RADIATION RESEARCH
0033-7587/10 $15.00

DOI: 10.1667/RR1899.1

An Adoptive Transfer Method To Detect Low-Dose Radiation-Induced Bystander Effects *In Vivo*

Benjamin J. Blyth,[a] Edouard I. Azzam,[b] Roger W. Howell,[b] Rebecca J. Ormsby,[1] Alexander H. Staudacher[a] and Pamela J. Sykes[a,c,1]

[a] *Haematology and Genetic Pathology, Flinders University, Bedford Park, South Australia 5042, Australia;* [b] *Department of Radiology, UMDNJ-New Jersey Medical School Cancer Center, Newark, New Jersey, 07103; and* [c] *SA Pathology, Flinders Medical Centre, Bedford Park, South Australia 5042, Australia*

Blyth, B. J., Azzam, E. I., Howell, R. W., Ormsby, R. J., Staudacher, A. H. and Sykes, P. J. An Adoptive Transfer Method To Detect Low-Dose Radiation-Induced Bystander Effects *In Vivo*.

The potential for irradiated cells to induce biological effects in their unirradiated neighbors (known as the bystander effect) has been observed repeatedly *in vitro*. However, whether bystander effects occur *in vivo* under the specific conditions relevant to low-dose radiation protection is still unclear. To test this, the fate of bystander cells in the mouse spleen was examined using an adoptive transfer method designed to replicate the rare, irradiated cells in an organ that might be expected after a low-dose-rate, low-LET radiation exposure. Splenic lymphocytes radiolabeled with low activities of ^{3}H-thymidine were introduced into the spleens of unirradiated recipient mice. In this study, the apoptotic and proliferative response of the neighboring bystander spleen cells was compared to the response of spleen cells in parallel control recipients that received sham-irradiated cells. Neither the local area surrounding lodged radiolabeled cells nor the spleen as a whole showed a change in apoptosis or proliferation either 1 or 3 days after adoptive transfer. Increasing the irradiated cell numbers, increasing the mean ^{3}H-thymidine activity per cell, or exposing cells *ex vivo* to an acute X-ray dose also had no effect. Possible reasons for the absence of a bystander effect in the spleen under these conditions are discussed.

INTRODUCTION

At radiation exposures above 100 mSv, carcinogenic risk can be determined directly from available epidemiology data (*1, 2*). For the purposes of radiation protection, the carcinogenic risk of radiation doses below 100 mSv is currently estimated on the premise that the risk remains linearly proportional to radiation dose down to background exposure levels (*3–5*). The actual risk posed by low-dose radiation might deviate from the risk predicted by such a linear no-threshold model, given the observation of two low-dose radiation phenomena, the radioadaptive response and radiation-induced bystander effects (*4, 6–9*). The adaptive response, originally described *in vitro* (*10–13*), has now also been observed *in vivo* for cancer end points at very low doses (0–100 mSv) (*14–19*). On the other hand, although radiation-induced bystander effects have been demonstrated clearly *in vitro*, the effect has yet to be shown *in vivo* for exposures in this low-dose range (*6, 20–25*).

The term radiation-induced bystander effects has been used to describe many different observations of intercellular communication after radiation exposure, both *in vitro* and *in vivo* (*6, 26*). While all of these effects might be conceptually related, not all phenomena described as bystander effects are relevant to the question of low-dose radiation risk, and they should not be considered interchangeably. When exposed to low fluences of photons and/or particulate radiations, in the range where carcinogenic risk is uncertain, isolated cells in a tissue can receive energy depositions that result in a wide range of absorbed doses in irradiated cells while neighboring bystander cells receive no energy deposition at all (*27–30*). Even with constant exposure to sparsely ionizing, low-LET radiation (100 kVp X rays) at 20 mSv per year [the occupational exposure limit (*31*)], the fraction of cells receiving any energy deposition within a 1-h period is $<0.25\%$ (*29*). It follows that to replicate exposures that result in the majority of cells remaining unirradiated, the dose to the irradiated cells should be equivalent to single electron tracks (of the order of a few mGy). The majority of bystander studies with low-LET radiations do not emulate these circumstances and fail to approximate single low-dose irradiated cells surrounded by unirradiated cells. When considering exposures to high-LET particles such as α particles emitted by radon progeny in the lung or from diagnostic nuclear medicine procedures, the dose delivered to an irradiated cell can exceed 100 mGy, but the proportion of irradiated cells

[1] Address for correspondence: Haematology and Genetic Pathology, Flinders University and SA Pathology, Flinders Medical Centre, Bedford Park, SA 5042, Australia; e-mail: pam.sykes@flinders.edu.au.

per unit dose can be considerably smaller. The technical difficulties associated with delivering low radiation doses to identifiable isolated cells within a living animal has proven to be a significant barrier to creating these conditions *in vivo*.

Therefore, we set out to develop a method for studying low-dose and low-dose-rate radiation-induced bystander effects *in vivo*. The system was designed to replicate the conditions relevant to determining the carcinogenic risk associated with exposure to low absorbed doses. The experiments were aimed at monitoring key factors that could alter carcinogenic risk (apoptosis and proliferation) in unirradiated cells within the mouse spleen when in the vicinity of single cells exposed to dose rates as low as ~3 mGy/h (~1 tritium disintegration per hour in 1/500 to 1/10,000 cells) or a single X-ray dose of 100 mGy (to ≈1/10,000 cells). This experimental system seeks to determine whether the wealth of low-dose *in vitro* bystander effect data that have been accumulated thus far can be observed *in vivo*.

MATERIALS AND METHODS

Mice

Male and female C57BL/6J mice were purchased from the University of Adelaide (Adelaide, Australia). Male and female pKZ1$^{-/-}$ and pKZ1$^{+/-}$ transgenic mice were obtained from an existing colony at Flinders Medical Centre (Adelaide, Australia). The pKZ1 transgenic mice, previously described in detail by Matsuoka *et al.* (*32*) and Sykes *et al.* (*33*), are bred on a C57BL/6J background and contain an *Escherichia coli lacZ* reporter gene to detect chromosomal inversions. For the purposes of these experiments, the pKZ1 mice are phenotypically equivalent to the C57BL/6J mice. Mice were group housed in micro-isolator cages with food and water provided *ad libitum*. The Flinders University Animal Ethics Welfare Committee approved all experiments.

Adoptive Transfer Method

The adoptive transfer method to introduce rare, irradiated cells into an unirradiated mouse spleen is outlined in Fig. 1. Donor splenic lymphocytes were irradiated either by incorporation of ^{3}H-thymidine or by acute irradiation with 6 MeV X rays. Irradiated donor cells or their sham-irradiated counterparts were labeled fluorescently and injected intravenously into unirradiated recipient mice.

1. ^{3}H-radiolabeled donor cells

Donor mice were killed humanely by CO_2 asphyxiation and spleens were isolated. Cells were expelled from the spleen by perfusing the spleen with RPMI medium [RPMI 1640 (CSL Limited, Australia) supplemented with 5% v/v FCS (Trace Scientific Ltd., Australia), L-glutamine (0.29 g/liter; Trace Scientific) penicillin (50 IU/ml; Trace Scientific), and streptomycin (50 μg/ml; Trace Scientific) and buffered with 0.21% w/v sodium bicarbonate] and gently massaging the capsule. Mononuclear cells were isolated from the cell suspension by underlaying with polysucrose/sodium ditrizoate solution at a density of 1.083 g/ml (Sigma-Aldrich Corp., St. Louis, MO) and centrifuging at 1050*g* for 10 min. Cells that collected at the polysucrose/medium interface were isolated and washed twice (380*g*, 10 min) in fresh RPMI medium.

T lymphocytes were obtained by negative selection with biotinylated monoclonal antibodies (CD11b, CD45R (B220), DX5 and Ter-119) against non-T-lymphocyte cell-surface markers (Pan T Cell Isolation Kit, Miltenyi Biotec GmbH, Germany) according to the manufacturer's instructions. The purity and specificity of the separation technique were measured by staining positively and negatively selected cell fractions with anti-CD90-FITC and anti-biotin-PE antibodies (Miltenyi Biotec) and analyzing by flow cytometry (FACScan™, Becton Dickinson, Franklin Lakes, NJ). Isolated T lymphocytes at 10^{6} cells/ml were microcultured in RPMI medium supplemented with a total of 10% v/v FCS and 50 μ*M* β-mercaptoethanol in 96-well plates. Cells were stimulated with 5 μg/ml concanavalin A (Sigma-Aldrich), and plates were incubated for 25 h in a humidified incubator (37°C, 10% CO_2 in air).

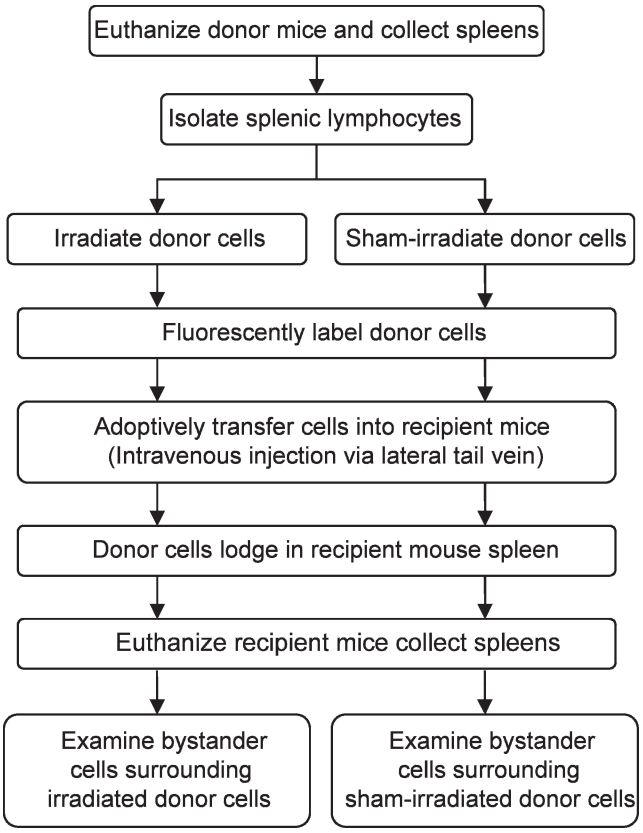

FIG. 1. Summary of adoptive transfer experimental method.

After the cultures were established, donor cells were radiolabeled with various activities of [methyl-^{3}H]-thymidine (37 MBq/ml, specific activity 3.18 TBq/mmol, GE Healthcare, WI) with control cells incubated in parallel with the equivalent molar concentration of unlabeled thymidine (Sigma-Aldrich). The intracellular-binding fluorescent dye CellTracker™ Orange CMRA (Invitrogen, Carlsbad, CA) resuspended in pure DMSO (BDH Merck, Australia) was simultaneously added to a final CMRA concentration of 2.5 μ*M*.

After 18 h exposure with ^{3}H-thymidine or unlabeled thymidine, sample wells were pulsed for 30 min in fresh RPMI medium containing 0.465 n*M* unlabeled thymidine. These cells were then centrifuged onto slides, fixed in 4% formaldehyde [from paraformaldehyde in PBS (pH 7.4), Sigma-Aldrich], dehydrated through graded ethanol, and dipped in fine-grain autoradiographic emulsion (Hypercoat EM-1, GE Healthcare). Slides were exposed at 4°C in the dark for 7 days and then immersed in D-19 developer (Eastman Kodak Co., NY) for 2 min, stopped in 1% acetic acid (BDH Merck), and cleared with Kodak Fixer (Eastman Kodak). Slides were mounted with fluorescence anti-fade medium containing 1.5 μg/ml 4′,6-diamidino-2-phenylindole (Vectashield® with DAPI, Vector Laboratories Inc., Burlingame, CA).

Incorporated radioactivity was quantified by liquid scintillation counting according to the method of Gerashchenko and Howell (*34*). Triplicate samples of pooled donor cell suspensions at the end of the labeling period were added to 5 ml of scintillation cocktail (Ready-Safe, Beckman Coulter, Inc., Fullerton, CA) in PolyQ vials (Beckman Coulter), and counts per minute in the ^{3}H counting window were read on an LS3801 liquid scintillation counter (Beckman Coulter). Parallel triplicate samples of supernatants remaining after centrifugation of the cell suspensions were also assayed, and the mean difference between the cell suspensions and their supernatants was compared to a prepared standard curve of ^{3}H-thymidine activities to measure the cell-associated ^{3}H activity. The quotient of total ^{3}H radioactivity and the number of radiolabeled cells in the sample (from the percentage of ^{3}H-positive cells determined by autoradiography) gave the average incorporated ^{3}H activity per radiolabeled cell (*35*). Radiolabeled or control donor cells for adoptive transfer were washed in fresh RPMI medium, then in PBS before final resuspension in PBS (200 µl per injection).

2. Acutely X-irradiated donor cells

Splenic mononuclear cells were isolated as for the chronic radiolabeling procedure above. The resulting mixed splenocytes were then cultured for 1 h in RPMI medium containing 10 µ*M* CellTracker™ Orange CMRA and then washed twice in mouse osmolarity buffered saline (*36*). Cells were resuspended at 2.5×10^6 cells/ml in tissue culture flasks and irradiated with 0.1 or 1 Gy X rays (5 Gy/min) using a Siemens Primus 6 MeV linear accelerator (Siemens Corporation, New York, NY) at the Adelaide Radiotherapy Centre (Flinders Private Hospital, Bedford Park, SA, Australia). Sham-irradiated control cells were treated in the same manner except that they were not exposed to the beam. A build-up layer of 1.4 cm depth of water equivalent (RW3) was placed above the flask, and MOSFET dosimeter calibrations reported a dose error of ± 3% (95% confidence).

3. Adoptive transfer

While under isofluorane anesthesia (2–3% isofluorane in oxygen delivered at 2 liters min^{-1}, VCA I.S.O., Veterinary Companies of Australia Pty Ltd, Australia), recipient mice were injected with 200 µl of cell suspension from the chronic radiolabeling or acute irradiation protocols via the lateral tail vein using a 29-gauge needle. After 1 or 3 days, recipient mice were killed humanely by CO_2 asphyxiation before the spleen was removed and snap-frozen on dry ice in cryoprotectant medium (Sakura Finetek Europe, B.V., the Netherlands) and then stored at −80°C.

Apoptosis and Proliferation Staining

Stored frozen spleen tissues were brought to −18°C and 5-µm sections were cut using a Reichart-Jung Cryocut 1800 cryostat (Leica Microsystems GmbH, Wetzlar, Germany). Sections were mounted onto 3-aminopropyltriethoxysilane-treated (Sigma-Aldrich) glass microscope slides. Apoptotic nuclei in recipient mouse spleens were visualized using the TdT-mediated dUTP nick end-labeling (TUNEL) method. Spleen sections were fixed for 30 min in 1% formaldehyde (from paraformaldehyde in PBS), permeabilized with 1% Triton X-100/1% sodium citrate dihydrate in PBS (Sigma-Aldrich Corp.), and labeled using an *In Situ* Cell Death Detection Kit (Roche Diagnostics GmbH, Penzberg, Germany) following the manufacturer's instructions. Labeling solution only (omitting enzyme) was used for negative control slides. Slides were mounted with Vectashield® with DAPI (Vector Laboratories Inc.) and stored in the dark at −20°C.

Proliferating cells in recipient mouse spleens were detected by staining for expression of the Ki-67 nuclear antigen. Spleen sections were fixed in 2% formaldehyde (from paraformaldehyde in PBS), permeabilized in 1% Triton X-100 in PBS, and incubated at 4°C overnight with rabbit anti-Ki-67 monoclonal antibody (Lab Vision Corp., Fremont, CA). Primary antibody was detected with a goat anti-rabbit IgG antibody conjugated with Alexa Fluor488® (Invitrogen). Primary and/or secondary antibody was omitted for negative control slides. Slides were mounted with Vectashield® with DAPI (Vector Laboratories Inc.) and stored in the dark at −20°C.

Fluorescence microscopy was performed using an Olympus Ax70 epifluorescence microscope (Olympus, Tokyo, Japan) fitted with a 16-bit cooled-CCD camera (Hamamatsu Photonics, KK, Japan) controlled by AnalySIS® FIVE software (Olympus). Unscaled 12-bit TIFF images were acquired for each field using a single exposure time that restricted fluorescence signals within the dynamic range of the camera. Images were analyzed using ImageJ v1.37a software (National Institutes of Health, Bethesda, MD). Deposited silver grains from autoradiography on cells or tissues were observed and photographed on the same microscope using bright-field illumination only. For analysis in three dimensions, slides mounted with 50-µm tissue sections (prepared and stained as above) were imaged on a Leica DMI6500B Inverted Microscope using a Leica TCS SP5 Spectral Confocal scanner/detector controlled by the Leica Application Suite Advanced Fluorescence v1.3.1 (Leica Microsystems).

1. Global screening

For evaluating global apoptosis frequency or global proliferation index, random fields (428 µm × 342 µm, 20× objective) throughout the spleen (maximum of 20 fields) were selected from each of two non-consecutive stained spleen sections per mouse, and multiple images were recorded using standard filter sets for DAPI, fluorescein and CMRA fluorochromes (Chroma Optical, Rockingham, VT). All slides were screened by the same observer, blinded to the identity of the mouse and its treatment group, which was decoded only after data collection was complete. For scoring apoptosis, the numbers of TUNEL-stained recipient spleen cells in each field were counted manually from pseudo-colored overlay images. Total cell numbers were estimated automatically using the ImageJ software from the proportion of the field positively stained with the DAPI nuclear counterstain. For quantifying proliferation, the proportion of the field that stained positive for Ki-67 was calculated automatically using the ImageJ software and expressed relative to the proportion of DAPI staining as above. The frequency of donor cell lodging in the spleen for each mouse was determined from the total number of CMRA-positive cells scored in each of the four sections examined divided by the total number of recipient spleen cells screened.

2. Local screening

For evaluating local apoptosis frequency or local proliferation index, fields (212 µm × 170 µm, 40× objective) containing CMRA-labeled donor cells were identified and multiple images were recorded using standard filter sets for DAPI, fluorescein and CMRA fluorochromes. Each field containing donor cells (up to a maximum of 25 fields) was analyzed for each of two stained spleen sections per mouse. When donor cells lodged near the outer edge of the spleen cross section, local fields were photographed only when the tissue section filled the entire field of view. When donor cells identified in a local screen also stained positive for Ki-67, this was noted and recorded. The apoptosis frequency and proliferation index were calculated using the same method as for the global screening. After each slide was screened, the slides were dehydrated through graded ethanol and processed for autoradiography as described above. The fields photographed earlier were then re-examined for deposited silver grains over the CMRA-labeled cells to confirm whether the chosen fields contained ^{3}H-labeled cells.

Data and Statistical Analysis

Data acquired for each photographed field were recorded in a statistical database using SPSS 15.0 for Windows (SPSS Inc., Chicago,

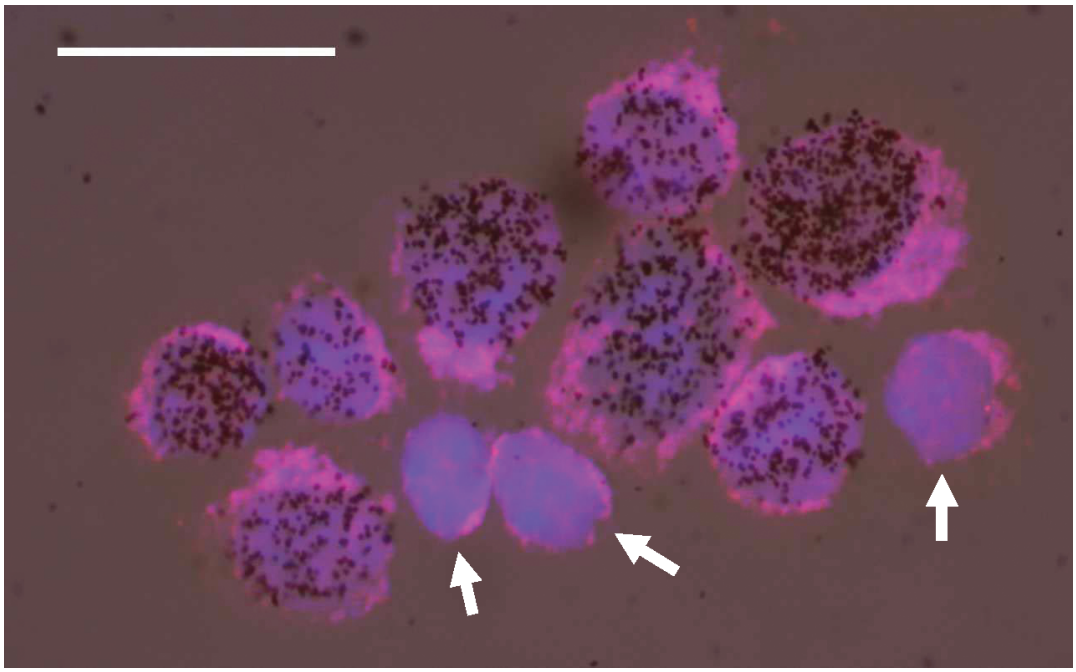

FIG. 2. Fluorescent staining and autoradiography of ^{3}H-radiolabelled donor cells. Donor T lymphocytes sampled at the end of the CellTracker™ Orange CMRA/^{3}H-thymidine incubation period were fixed and processed for autoradiography. Epifluorescence and bright-field microscopy revealed cells with positive cytoplasmic CMRA staining (red) with DAPI-counterstained nuclei (blue) that have either incorporated ^{3}H-thymidine and have visible autoradiography grains (black) or did not incorporate the radiolabel and are free of deposited silver grains (arrows). Scale bar shows 25 μm.

IL). Apoptosis frequencies and proliferation indices are all presented as sample means ± 95% confidence intervals to indicate the spread of the data between recipient mice. All other data presented are shown as means ± SD. Sample means were compared between two groups using the Independent Student's *t* test (two-tailed) or across more than two groups using ANOVA (two-tailed). Linear correlations were tested using Spearman's rank correlation coefficients. For all tests, statistical significance was reached when $P < 0.05$.

RESULTS

Validation of Adoptive Transfer Method

In five separate ^{3}H-thymidine radiolabeling experiments, spleen T lymphocytes isolated from at least five donor mice were pooled and stimulated to proliferate in the presence of 1.48 kBq ml^{-1} [methyl-^{3}H]-thymidine and CellTracker™ Orange CMRA fluorescent probe. During the 18-h radiolabeling periods, an average of 74 ± 6% of nuclei incorporated the ^{3}H-thymidine (Fig. 2), and all cells were fluorescently labeled with the cell tracing probe. The radiolabeled cells incorporated a mean radioactivity of 0.30 ± 0.04 mBq (approximately one ^{3}H decay per hour, Table 1) with each decay calculated to deliver a nominal absorbed dose of 2.61 mGy to the cell nucleus (*35*) modeled on a spherical nucleus with a radius of 4 μm.

Under all conditions tested, fluorescently labeled donor cells injected intravenously into unirradiated mice could be observed 1 to 3 days later in 5-μm-thick frozen sections cut from the recipient mouse spleens (Fig. 3). As expected, donor T lymphocytes were found to be lodged nonrandomly, with a tendency to lodge in the periarteriolar lymphoid sheaths, although it was rare to observe several donor cells within a single field (Fig. 4A). When increased numbers of cells were injected, this same preferential lodging could be observed as clusters of donor cells, with hundreds of fluorescently labeled cells lodged within a radius of several hundred micrometers (Fig. 4B). These donor cell clusters could also be visualized in three dimensions using confocal microscopy (Fig. 5). Lodged donor cells were still brightly labeled and were easily identifiable in tissues stored at −80°C for more than a year. The fluorescent probe was resistant to formaldehyde fixation and could survive ethanol dehydration, autoradiography processing, enzymatic labeling and immunohistochemistry protocols.

Analysis of Apoptosis and Proliferation in Bystander Cells Surrounding Low-Dose-Rate Radiolabeled Cells

Spleen T lymphocytes pooled from five C57BL/6J donor mice were radiolabeled with 1.48 kBq ml^{-1} ^{3}H-thymidine or sham-radiolabeled with the equivalent molar concentration (0.465 n*M*) of non-radioactive thymidine. After the radionuclide labeling, 69 ± 5% of donor cells had incorporated a mean radioactivity of 0.33 ± 0.02 mBq cell^{-1} (Table 2). Over three replicate

TABLE 1
Dosimetry for Chronic Radiolabeling of Donor Cells

Experiment	^{3}H-positive cells (%)	Incorporated radioactivity (mBq cell^{-1})	Nuclear absorbed dose rate (mGy h^{-1})
1	73	0.34	3.2
2	65	0.32	3.0
3	72	0.32	3.0
4	81	0.23	2.2
5	77	0.31	2.9
Mean	74	0.30	2.9
Standard deviation	6	0.04	0.4

experiments, four to six C57BL/6J recipient mice were injected with either 5×10^5 radiolabeled or sham-radiolabeled donor cells and the recipient mouse spleens were isolated and cryopreserved 22 h later. There was no significant difference in donor cell lodging between the sham-labeled and radiolabeled donor cell recipient mouse groups ($P = 0.4$) or across the triplicate experiments ($P = 0.4$, ANOVA). In the mice receiving radiolabeled cells, 64 ± 6% of the donor cells identified as lodged in the spleen were positive for incorporated ^{3}H-thymidine by autoradiography, which was not significantly lower than before injection ($P > 0.2$). Apoptosis and proliferation were measured in recipient spleen cells (bystander cells) in the area surrounding lodged donor cells (local screening, Fig. 6a, c) and randomly throughout the spleen sections (global screening, Fig. 6b, d).

There was no difference in the levels of apoptosis ($P = 0.3$, Fig. 7) or proliferation ($P = 0.5$, Fig. 8) between unirradiated bystander cells surrounding radiolabeled cells and those surrounding sham-radiolabeled donor cells (local screen). Likewise, there was no difference in apoptosis ($P = 0.5$) or proliferation ($P = 0.6$) of bystander cells throughout the spleen (global screen) between mice receiving radiolabeled cells and those injected with sham-radiolabeled cells (Table 2). In the mice receiving radiolabeled donor cells, there was no difference in the apoptosis frequency ($P = 0.6$) or proliferation index ($P = 0.2$) between local fields containing autoradiography-confirmed ^{3}H-positive donor cells and those that contained ^{3}H-negative donor cells. Similarly, there was no significant correlation between local apoptosis frequency ($P = 0.35$, Spearman's) or local proliferation index ($P = 0.06$, Spearman's) and the number of autoradiography-confirmed ^{3}H-positive donor cells per field.

When two more experiments were performed under the same conditions, but with analysis 72 h after adoptive transfer into pKZ1$^{+/-}$ recipient mice, there was again no difference in the apoptosis frequency or proliferation index of unirradiated recipient cells between spleens receiving radiolabeled cells and those receiving sham-radiolabeled control cells using either the local or global screening method (Table 3). After 3 days of ^{3}H-thymidine exposure *in vivo*, the percentage of surviving donor cells confirmed to be ^{3}H-positive by autoradiography was only 21 ± 8%, down from 77% before adoptive transfer.

These experiments used pKZ1 recipient mice to allow the future examination of chromosomal inversions as an end point in bystander tissues (data not shown). The baseline apoptosis frequency was 66% higher in the pKZ1 mice than the C57BL/6J mice ($P < 10^{-6}$); however, since the spontaneous apoptosis frequency in both mouse groups was so low (<0.7%), the difference actually represents less than three extra apoptotic cells per thousand. The rate of proliferation was equivalent in both mouse groups ($P = 0.55$).

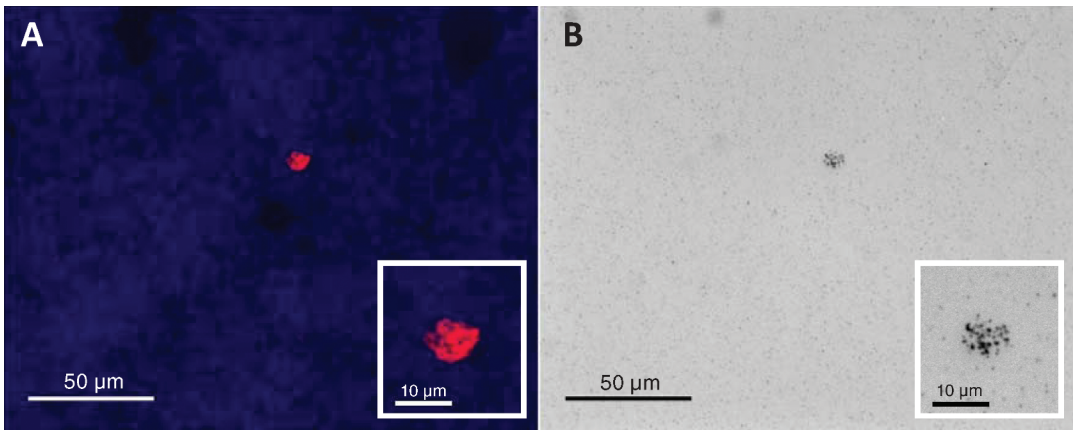

FIG. 3. Fluorescent staining and autoradiography of a ^{3}H-radiolabeled donor cell lodged in a recipient mouse spleen. Frozen sections (5 µm) of recipient mouse spleen were examined under fluorescence and bright-field microscopy. Panel A: Fluorescently labeled donor cells (red) were identified and photographed along with the surrounding DAPI-counterstained spleen cells (blue). Panel B: Slides were then processed for autoradiography and the same field was re-examined. The majority of the lodged donor cells exhibited deposited silver grains over the cell nucleus (see insets).

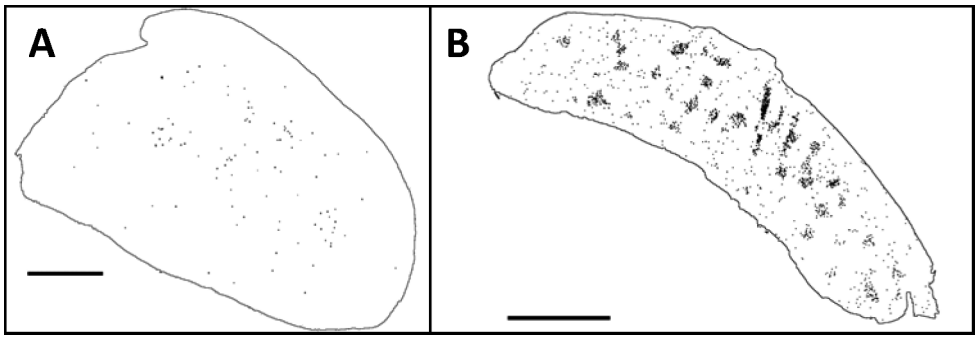

FIG. 4. Lodging pattern of donor cells within recipient mouse spleens. Single 5-μm spleen sections from recipient mice taken 1 day after injecting 5×10^5 (panel A) or 5×10^6 (panel B) sham-treated donor cells were viewed by fluorescence microscopy and photographed with multiple overlapping fields using filter sets to visualize the DAPI nuclear counterstain and the CMRA-labeled donor cells. The multiple images were reconstructed to form a montaged image of the entire spleen section, and the outline of the cross section and the locations of lodged CMRA-positive cells was recorded (locations marked, markers not to scale). Scale bars show 1 mm.

Analysis of Apoptosis and Proliferation in Bystander Cells Surrounding Increased Numbers of Low-Dose-Rate Radiolabeled Cells

To simulate an increasing proportion of irradiated cells, recipient pKZ1$^{+/-}$ mice were injected with 5×10^6 radiolabeled donor cells or sham-radiolabeled control cells prepared as described above, with analysis 22 h later (Table 4). There was no difference in the apoptosis frequency or proliferation index between spleens receiving radiolabeled cells and those receiving sham-radiolabeled control cells. The proportion of ^{3}H-positive donor cells lodged in the spleen was 66 ± 7%, significantly lower than the radiolabeling frequency of the donor cells before injection ($P = 0.003$). Since local fields containing single donor cells were rare due to the high density of donor cell lodging, apoptosis and proliferation in the bystander cells were using only the global screening method.

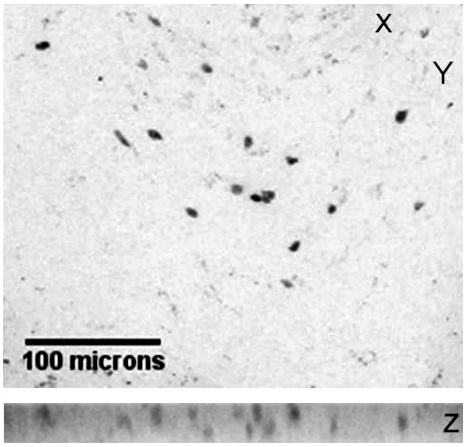

FIG. 5. Clustered lodging of donor cells within a recipient mouse spleen. Clusters of lodged donor cells in 50-μm frozen spleen sections from recipient mice 1 day after injecting with 5×10^5 sham-treated donor cells were identified by confocal microscopy. A z-series imaging CMRA fluorescence was taken at 1.5-μm intervals through the depth of the section to a total depth of 30 μm. The mean fluorescence intensity through the stack was projected into a composite image (shown at top) and the color was inverted for clarity (fluorescence intensity increasing from white to black). Numerous CMRA-positive cells (black) can be seen within the field. The same stack viewed side-on (shown at bottom) shows that the lodged donor cells are not present in a single plane but form a three-dimensional cluster that likely extends several hundred micrometers above and below the frozen section. Scale bars show 100 μm.

Analysis of Apoptosis and Proliferation in Bystander Cells Surrounding High-Dose Irradiated Cells

As a positive control, recipient pKZ1$^{+/-}$ mice were injected with 5×10^5 donor cells radiolabeled with 74 kBq ml^{-1} ^{3}H-thymidine (50-fold higher than in previous experiments) or sham-radiolabeled with the equivalent molar concentration of nonradioactive thymidine (23.25 n*M*) and analyzed 22 h after adoptive transfer (Table 5). When the [methyl-^{3}H]-thymidine activity of the culture medium was increased to 74 kBq ml^{-1}, only 51% of donor cells incorporated the ^{3}H-thymidine to a mean activity of 28 mBq cell^{-1} (approximately 100 ^{3}H decays per hour).

There were 70% fewer donor cells lodged in the spleens of mice receiving high-dose radiolabeled cells compared to those receiving sham-radiolabeled cells ($P < 10^{-7}$), and only 5 ± 4% of the remaining cells were positive for ^{3}H by autoradiography. There was no significant difference in apoptosis ($P = 0.7$) or proliferation ($P = 0.99$) of bystander cells in the spleens of mice between the two recipient mouse groups. Since so few of the remaining lodged donor cells were ^{3}H-positive, there were too few fields with confirmed ^{3}H-positive donor cells to compare local screening results for either end point.

As a further positive control experiment, C57BL/6J mice were injected with 5×10^5 X-irradiated (0.1 or

TABLE 2
Bystander End Points in Recipient Mice Analyzed 22 h after Receiving 5×10^5 Donor Cells

	Donor cells received		
	Sham-radiolabeled	Radiolabeled	*P*
C57BL/6J recipient mice (*n*)	13	15	—
Donor cell radiolabeling (%)[a]	—	69 ± 5	—
Donor cell radioactivity (mBq cell^{-1})[a]	—	0.33 ± 0.02	—
Lodging frequency ($\times 10^{-4}$)[a]	1.6 ± 0.8	1.4 ± 0.6	0.36
$^3H^+$ donor cells *in situ* (%)[a]	—	64 ± 6	—
Local apoptosis frequency ($\times 10^{-3}$)[b]	3.8 ± 0.5	3.4 ± 0.4	0.3
Global apoptosis frequency ($\times 10^{-3}$)[b]	2.8 ± 0.5	2.6 ± 0.5	0.5
Local proliferation index (%)[b]	9.5 ± 0.9	9.2 ± 0.6	0.5
Global proliferation index (%)[b]	10.7 ± 2.3	10.1 ± 0.8	0.6

[a] Standard deviation.
[b] ± 95% CI.

1 Gy) or sham-irradiated mixed spleen lymphocytes and analyzed 22 h after adoptive transfer. The donor cell lodging frequency was significantly reduced ($P = 0.037$, Bonferroni-corrected post-hoc *t* test) in the mice receiving the donor cells irradiated with 1 Gy (Table 6). There was no difference in the apoptosis frequency ($P > 0.5$) or proliferation index ($P > 0.3$) of bystander recipient cells between mice receiving irradiated cells and those receiving sham-irradiated control cells using either the local or global screening method (Table 6).

DISCUSSION

Here we present the first results from an *in vivo* system analyzing apoptosis and proliferation in normal, unirradiated spleen cells in response to the presence of

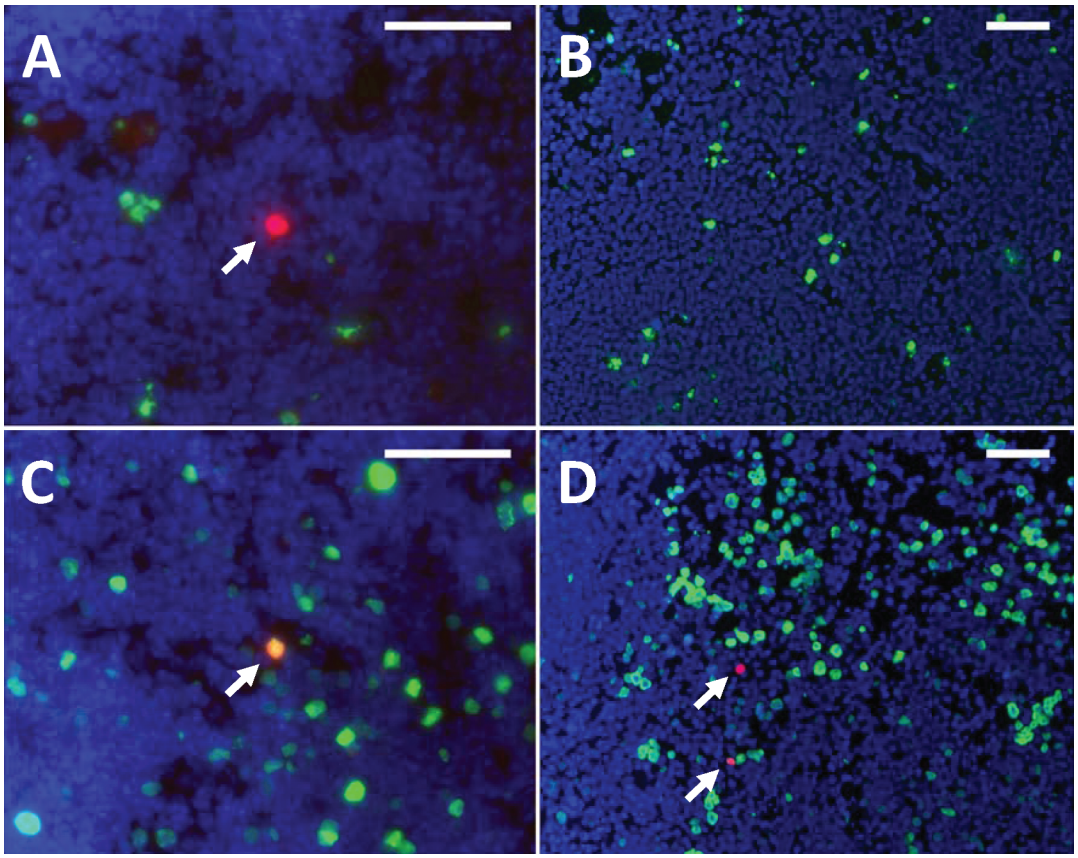

FIG. 6. Staining for bystander end points in recipient mouse spleens. Representative fields from spleen sections of recipient mice stained (green) for apoptosis (panels A and B) and proliferation (panels C and D). Bystander recipient cells are counterstained with DAPI (blue). Local fields (panels A and C) are centered on lodged donor cells (red, arrowed) while global fields are selected randomly and may contain no donor cells (panel B) or one or multiple donor cells (panel D). Scale bars show 50 μm.

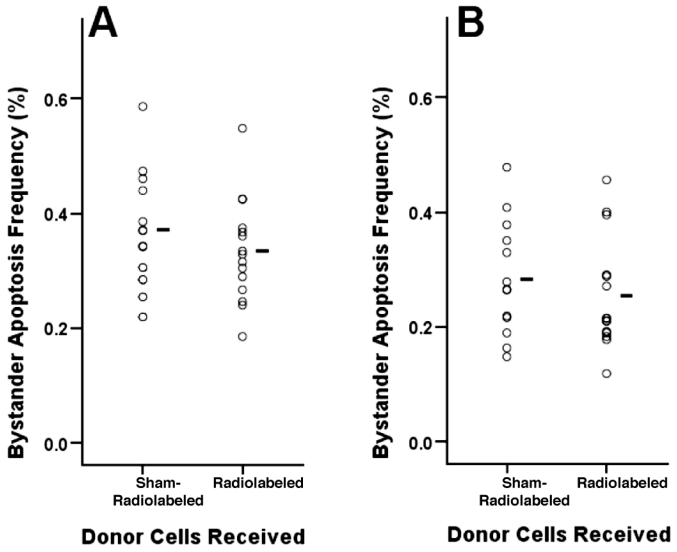

FIG. 7. Bystander apoptosis in recipient mouse spleens. The frequency of TUNEL-positive apoptotic cells in the immediate area surrounding lodged donor cells (local screen, panel A) or throughout the spleen tissue (global screen, panel B) is shown for mice receiving sham-radiolabeled or radiolabeled donor cells. Apoptosis frequencies from individual mice are marked with open circles (○) and the group means are shown by a bar (–).

neighboring cells receiving radiation energy depositions *in situ*. This *in vivo* adoptive transfer method has proven to be robust, reproducible and flexible enough to allow study of variations in exposure time, dose rate, radiation source and the ratio of irradiated to unirradiated cells in the tissue. The doses and dose rates in this study were chosen to mimic bystander scenarios relevant to

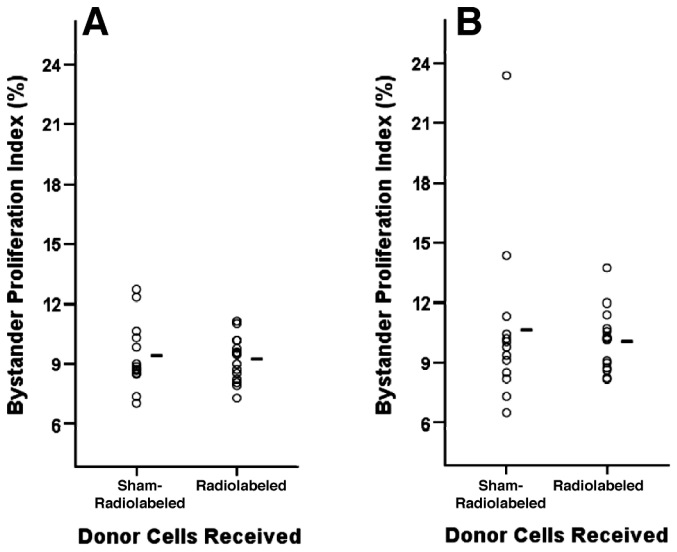

FIG. 8. Bystander proliferation in recipient mouse spleens. The percentage of Ki-67-positive proliferating cells in the immediate area surrounding lodged donor cells (local screen, panel A) or throughout the spleen tissue (global screen, panel B) is shown for mice receiving sham-radiolabeled or radiolabeled donor cells. Proliferation indices from individual mice are marked with open circles (○) and the group means are shown by a bar (–).

TABLE 3
Bystander End Points in Recipient Mice Analyzed 72 h after Receiving 5×10^5 Donor Cells

	pKZ1$^{-/-}$ donor cells received		
	Sham-radiolabeled	Radiolabeled	*P*
pKZ1$^{+/-}$ recipient mice (*n*)	17	16	—
Donor cell radiolabeling (%)	—	77	—
Donor cell radioactivity (mBq cell^{-1})	—	0.31	—
Lodging frequency ($\times 10^{-4}$)[a]	0.9 ± 0.6	0.9 ± 0.5	0.9
$^3H^+$ donor cells *in situ* (%)[a]	—	21 ± 8	—
Local apoptosis frequency ($\times 10^{-3}$)[b]	6.3 ± 1.2	6.4 ± 1.8	0.8
Global apoptosis frequency ($\times 10^{-3}$)[b]	5.2 ± 0.8	5.1 ± 1.0	0.8
Local proliferation index (%)[b]	9.3 ± 0.9	9.4 ± 1.9	0.95
Global proliferation index (%)[b]	11.9 ± 2.5	13.4 ± 2.8	0.4

[a] ± Standard deviation.
[b] ± 95% CI.

radiation protection at low doses, and apoptosis and proliferation were chosen as end points because they represent key modifiers of carcinogenic risk and allow comparison with published *in vitro* bystander data; however, almost any fluorescence end point could be measured in these tissues using this method.

This report is the first to use adoptive transfer of lymphocytes to introduce irradiated cells into an intact unirradiated organ of a physiologically normal animal to study radiation-induced cell-cell interactions. Other methods aimed at detecting bystander effects *in vivo*

TABLE 4
Bystander End Points in Recipient Mice Analyzed 22 h after Receiving 5×10^6 Donor Cells

	pKZ1$^{-/-}$ donor cells received		
	Sham-radiolabeled	Radiolabeled	*P*
pKZ1$^{+/-}$ recipient mice (*n*)	5	6	—
Donor cell radiolabeling (%)	—	81	—
Donor cell radioactivity (mBq cell^{-1})	—	0.23	—
Lodging frequency ($\times 10^{-4}$)[a]	18 ± 11	26 ± 9	0.24
$^3H^+$ donor cells *in situ* (%)[a]	—	66 ± 7	—
Global apoptosis frequency ($\times 10^{-3}$)[b]	5.0 ± 0.6	5.5 ± 1.3	0.6
Global proliferation index (%)[b]	11.6 ± 2.6	14.68 ± 4.0	0.25

[a] ± Standard deviation.
[b] ± 95% CI.

TABLE 5
Bystander End Points in Recipient Mice Analyzed 22 h after Receiving 5×10^5 High-Dose Radiolabeled Donor Cells

	$pKZ1^{-/-}$ donor cells received		
	Sham-Radiolabeled	Radiolabeled	*P*
$pKZ1^{+/-}$ recipient mice (*n*)	6	5	—
Donor cell radiolabeling (%)	—	51	—
Donor cell radioactivity (mBq $cell^{-1}$)	—	27.5	—
Lodging frequency ($\times 10^{-4}$)[a]	2.2 ± 0.2	0.6 ± 0.2	<0.001
$^3H^+$ donor cells *in situ* (%)[a]	—	5 ± 4	—
Global apoptosis frequency ($\times 10^{-3}$)[b]	6.5 ± 1.5	6.8 ± 0.6	0.7
Global proliferation index (%)[b]	10.8 ± 3.4	10.9 ± 3.5	0.99

[a] ± Standard deviation.
[b] ± 95% CI.

introduced both the irradiated and unirradiated cells into an immunodeficient or lethally irradiated host (*37–40*). Adoptively transferred splenic lymphocytes rapidly leave the circulation and lodge in the spleen in a highly reproducible and well-characterized pattern (*41*) that follows the behavior of normal circulating lymphocytes (*42, 43*). The spleen thus provides an ideal environment for monitoring interactions of identifiable transplanted cells with the indigenous tissue microenvironment. The donor lymphocytes in this study were stimulated *ex vivo* to divide to incorporate ^{3}H-thymidine into the DNA. However, these lectin-stimulated primary cells still reproduce a state much closer to normal *in vivo* homeostasis (splenic T lymphocytes are naturally highly proliferative *in vivo*) than tumor cells routinely used in bystander experiments. Other bystander experiments that use non-tumor cells are often stimulated with steroids to proliferate in culture (*44, 45*), which is known to up-regulate the expression of gap-junction proteins (*46*). The requirement for medium supplementation with β-mercaptoethanol to stabilize the *in vitro* oxidative environment [a role normally performed by macrophages *in vivo* (*47*)] further demonstrates the inability of *in vitro* cell monocultures to fully recapitulate an *in vivo* microenvironment. Despite the *ex vivo* culture and manipulation, the lodging of donor splenocytes in the present study appeared to follow the normal pattern observed for adoptively transferred splenocytes injected immediately without *ex vivo* culture (*42, 43*).

By carefully controlling the culture conditions, consistent nuclear absorbed doses from DNA-incorporated ^{3}H-thymidine could be achieved in the donor T lymphocytes using the method described in this report. At the lower concentrations of radioactivity reported here, no growth inhibition of donor cells during radiolabeling was detected relative to sham-radiolabeled cells, and both cell populations showed equivalent lodging after 22 or 72 h *in vivo*. Although not all donor cells divided *ex vivo* to incorporate radiolabel, we have demonstrated that in mice receiving ^{3}H-thymidine-labeled donor cells, those fields containing lodged ^{3}H-negative donor cells can be identified and excluded from analysis (if desired) or can be used as internal controls comparing the effect of irradiated and unirradiated donor cells lodged within the same spleen. The short-range β particles emitted by ^{3}H decay allow the repeated irradiation of single nuclei *in situ*, with each decay commensurate with electron traversal(s). It is thus important to note that the time elapsed since adoptive transfer is not to be equated to the time after the bystander signal because the irradiation occurs throughout the time the donor cells spend *in situ*.

At the lower number of transferred donor cells used in this study, organ-averaged donor cell lodging frequencies were of the order of 1–2 donor cells per 10,000 bystander spleen cells by 22 h after injection. This level corresponds to the fraction of spleen cells that might be exposed to an electron traversal within 1 h at a dose rate of 2 mSv of low-LET radiation per year (*27, 29, 30, 48, 49*). Few bystander effect experiments performed to date have approached the irradiated-to-unirradiated cell ratios that are relevant to low-dose radiation protection. Data from irradiated cell-conditioned medium transfer experiments on bystander dose responses predict that the effects are unlikely to be produced until low-LET

TABLE 6
Bystander End Points in Recipient Mice Analyzed 22 h after Receiving 5×10^5 X-Irradiated Donor Cells

	Donor cells received			
	0 Gy	0.1 Gy	1 Gy	P^a
C57BL/6J recipient mice (*n*)	8	6	6	–
Lodging frequency ($\times 10^{-4}$)[b]	0.6 ± 0.2	0.6 ± 0.2	0.4 ± 0.1	0.025
Local apoptosis Frequency ($\times 10^{-3}$)[c]	4.1 ± 0.8	4.4 ± 0.9	4.2 ± 0.8	0.9
Global apoptosis Frequency ($\times 10^{-3}$)[c]	3.0 ± 0.3	3.3 ± 0.5	3.3 ± 0.5	0.5
Local proliferation index (%)[c]	10.9 ± 1.4	11.2 ± 1.4	9.9 ± 1.0	0.3
Global proliferation index (%)[c]	11.3 ± 1.2	12.6 ± 2.0	11.1 ± 1.4	0.4

[a] ANOVA.
[b] ± Standard deviation.
[c] ± 95% CI.

radiation doses rise to levels at which all cells in the population are irradiated (*45, 50, 51*). Gerashchenko and Howell found that at least 50% of the cell population had to be radiolabeled with tritiated thymidine for the bystander effect to be observed (*16*). The potential relevance of bystander effects *in vivo* will likely be inversely related to the proportion of irradiated cells required to induce the effect; as more cells are irradiated, fewer unirradiated cells remain at risk. Extrapolations of bystander effects from very high proportions of irradiated cells down to the sparse cell irradiations relevant to low-dose radiation protection should be regarded with caution, since the toxic bystander signal generated by 600,000 cells irradiated at 500 mGy has been shown to be negated when the conditioned medium was diluted by only 1.2-fold and even at very high doses (5 Gy) was abolished by only a twofold dilution (*52*).

The density of donor cell lodging in the spleen is likely to have peaked prior to analysis at 22 h, and the relative reduction in donor cell lodging seen in the mice analyzed 3 days after injection is consistent with a gradual redistribution of transferred T cells from the spleen to the lymph nodes (*53, 54*). Although transferring 5×10^6 donor lymphocytes is at the level previously reported to result in saturation of spleen lodging sites (*54*), no decrease in the relative lodging frequency was observed compared with those experiments where 5×10^5 cells were transferred. Although this level may be approaching the upper limit possible with this technique, these findings suggest that it is possible to achieve organ-averaged lodging frequencies of at least one donor cell per 500 recipient cells.

Using the local screening method, it was possible to narrow our analysis to the immediate region surrounding lodged donor cells such that up to 1 in 50 cells within the field of view were irradiated donor cells. Since the spatial distribution of irradiated and bystander cells remains intact using our *in situ* analysis method, the range of analysis could potentially be restricted further to only cells adjacent to irradiated donor cells. It was also possible to test for a correlation between the number of donor cells in a field and the bystander apoptosis and proliferation levels to detect the effect of increasing ratios of irradiated to bystander cells. The homeostatic levels of apoptosis and proliferation differ for the various cell types within the spleen (*55*). The local screening method was deliberately biased toward the donor cell-rich areas, which are populated mainly by T lymphocytes. As such, the apoptosis frequency measured in the local screens was consistently higher than that measured in the global screens, which surveyed the full distribution of cell types within the spleen. The same effect was observed for proliferation, with T-lymphocyte-populated areas surveyed in the local screen showing lower baseline levels than when proliferation was measured across the whole spleen. These differences were seen in both recipient mouse groups consistently across all the experiments, with the local and global measurements highly correlated for both end points ($P < 10^{-3}$).

Unlike many published *in vitro* findings, the results presented here show no evidence for a significant change in either the apoptosis or proliferation of bystander cells *in vivo* 1 or 3 days after adoptive transfer. In the first experiments where bystander cells were analyzed after 22 h, the levels of both end points were no higher in the mice receiving radiolabeled donor cells compared to the controls, and the 95% confidence limits exclude an increase in apoptosis of more than 9% and an increase in proliferation of more than 18%. Analysis of bystander cells after 3 days showed apoptosis and proliferation in local bystander cells differing by less than 2% from the controls. Since apoptosis in the recipient mouse spleens was under *in vivo* homeostatic regulation and was measured *in situ*, the baseline levels were very low ($<0.7\%$) such that even a 10% change from baseline only would equate to less than one apoptotic cell in 1000 recipient bystander cells. The local screening method described here surveyed between 34,000 and 56,000 bystander spleen cells per mouse and the global screening method $>160{,}000$ cells per mouse, ensuring adequate precision to detect small changes. To put this sensitivity into context with effect sizes routinely observed *in vitro*, induction of bystander apoptosis is reported at levels from 100% above controls (*44–47*) to greater than 10-fold above controls (*56–59*). *In vivo*, however, common environmental stressors such as heat, diet, circadian rhythm and physical restraint are known to alter apoptosis and proliferation in the spleen to much greater extents than the differences observed between sham and bystander treatment groups in this study (*60–67*).

In the very low-dose range relevant to human exposures, increasing the average absorbed dose to a tissue results in an increasing fraction of irradiated cells within a tissue, although the dose received by most exposed cells continues to occur from single ionizing particle traversals. When this was simulated using the adoptive transfer model (by injecting 10-fold more radiolabeled cells per mouse), there was still no significant difference in bystander apoptosis or proliferation from the controls. Although outside the limits of natural low-LET radiation bystander scenarios, the adoptive transfer experiments were also repeated with a dose commensurate with those used in many *in vitro* bystander experiments as well as with single high-dose exposures to X rays. Surprisingly, the high-dose-rate ^{3}H, even though lethal to the radiolabeled cells, still did not significantly alter the apoptosis ($<5\%$ difference) or proliferation ($<1\%$ difference) of the unirradiated cells in the spleen. Likewise, bystanders to donor cells that received an acute *ex vivo* X-ray dose of 0.1 or 1 Gy showed no significant apoptotic or proliferative response.

Low-LET radiation has previously been shown to be effective at inducing bystander effects *in vitro* for a range of radiation energies and biological end points (*34, 45, 68–72*). The absence of a bystander effect in the mouse spleen in this study was surprising, given that the experiments were designed to simulate bystander scenarios relevant to radiation protection and were also tested with parameters chosen to mimic published *in vitro* studies. It is possible that bystander effects may be occurring *in vivo* in the spleen, albeit on a different time scale or at much lower magnitudes than those observed in *in vitro* experiments. Likewise, the *in vivo* responses of unirradiated cells in the spleen to their irradiated neighbors may be of a different nature than those observed previously *in vitro*.

Work that has been conducted to evaluate mouse strain dependence for bystander signaling suggests that tissues from C57BL/6J mice (as used in this study) did produce a medium-transferable bystander apoptosis signal (*73*) whereas mice from the radiation-sensitive CBA/Ca strain did not. The converse has been reported for genomic instability bystander effects (*74*), although genomic instability was not induced in the directly irradiated cells from either strain, even at the very high γ-radiation dose used (4 Gy). The limited *in vitro* data suggest that the human population may exhibit considerable variability in their ability to initiate or respond to bystander signals (*75, 76*), and as such, further investigation of bystander effects *in vivo* should include a range of representative genetic backgrounds.

Clearly, data from a vast array of experimental systems, cell types, dose ranges and biological end points support the potential of irradiated cells to communicate effects to unirradiated cells. However, it may be that the conditions required to generate bystander events *in vitro* (e.g. dose, dose rate and the ratio of irradiated to unirradiated cells) cannot be generalized to the *in vivo* low-dose external exposures of concern to regulators. Alternatively, it is possible that the variable and stochastic nature of bystander effects, as observed *in vitro*, may also result in tissue- and end point-specific findings *in vivo*. Future experiments will need to continue to explore a range of tissues, doses, environmental conditions and time scale for expression of biological effects to fully probe the potential of bystander signaling *in vivo*. The results of this study suggest that if bystander effects are occurring in the spleen *in vivo*, the magnitude of the effects may be less than those observed *in vitro* and that they may not pose as large a concern to radiation risk estimation as *in vitro* studies might predict.

ACKNOWLEDGMENTS

The authors wish to acknowledge Dr. David Turner and Dr. Keryn Williams for helpful discussions and the staff of the Flinders Medical Centre Animal House and Ms. Ami-Louise Cochrane for assistance with animal care and technical procedures. This work was funded by the Low Dose Radiation Research Program, Biological and Environmental Research, United States Department of Energy, Grant no. DE-FG02-05ER64104.

Received: June 22, 2009; accepted: October 1, 2009

REFERENCES

1. D. A. Pierce and D. L. Preston, Radiation-related cancer risks at low doses among atomic bomb survivors. *Radiat. Res.* **154**, 178–186 (2000).
2. D. L. Preston, E. Ron, S. Tokuoka, S. Funamoto, N. Nishi, M. Soda, K. Mabuchi and K. Kodama, Solid cancer incidence in atomic bomb survivors: 1958–1998. *Radiat. Res.* **168**, 1–64 (2007).
3. National Research Council, Committee to Assess Health Risks from Exposure to Low Levels of Ionizing Radiation, *Health Risks from Exposure to Low Levels of Ionizing Radiation: BEIR VII – Phase 2*. National Academies Press, Washington, DC, 2006.
4. ICRP, *Low-Dose Extrapolation of Radiation Related Cancer Risk*. Publication 99, *Annals of the ICRP*, Vol. 35, Elsevier, Amsterdam, 2006.
5. UNSCEAR, *Sources and Effects of Ionizing Radiation*, Vol. 2. United Nations, New York, 2000.
6. W. F. Morgan and M. B. Sowa, Non-targeted bystander effects induced by ionizing radiation. *Mutat. Res.* **616**, 159–164 (2007).
7. W. F. Morgan, Will radiation-induced bystander effects or adaptive responses impact on the shape of the dose response relationships at low doses of ionizing radiation? *Dose Response* **4**, 257–262 (2006).
8. R. J. Preston, Bystander effects, genomic instability, adaptive response, and cancer risk assessment for radiation and chemical exposures. *Toxicol. Appl. Pharmacol.* **207**, 550–556 (2005).
9. H. Nikjoo and I. K. Khvostunov, A theoretical approach to the role and critical issues associated with bystander effect in risk estimation. *Hum. Exp. Toxicol.* **23**, 81–86 (2004).
10. G. Olivieri, J. Bodycote and S. Wolff, Adaptive response of human lymphocytes to low concentrations of radioactive thymidine. *Science* **223**, 594–597 (1984).
11. J. K. Wiencke, V. Afzal, G. Olivieri and S. Wolff, Evidence that the [^{3}H]thymidine-induced adaptive response of human lymphocytes to subsequent doses of X-rays involves the induction of a chromosomal repair mechanism. *Mutagenesis* **1**, 375–380 (1986).
12. J. D. Shadley, V. Afzal and S. Wolff, Characterization of the adaptive response to ionizing radiation induced by low doses of X rays to human lymphocytes. *Radiat. Res.* **111**, 511–517 (1987).
13. S. Wolff, V. Afzal, J. K. Wiencke, G. Olivieri and A. Michaeli, Human lymphocytes exposed to low doses of ionizing radiations become refractory to high doses of radiation as well as to chemical mutagens that induce double-strand breaks in DNA. *Int. J. Radiat. Biol.* **53**, 39–47 (1988).
14. D. Bhattacharjee, Role of radioadaptation on radiation-induced thymic lymphoma in mice. *Mutat. Res.* **358**, 231–235 (1996).
15. Y. Ina and K. Sakai, Prolongation of life span associated with immunological modification by chronic low-dose-rate irradiation in MRL-lpr/lpr mice. *Radiat. Res.* **161**, 168–173 (2004).
16. Y. Ina and K. Sakai, Further study of prolongation of life span associated with immunological modification by chronic low-dose-rate irradiation in MRL-lpr/lpr mice: effects of whole-life irradiation. *Radiat. Res.* **163**, 418–423 (2005).
17. Y. Ina, H. Tanooka, T. Yamada and K. Sakai, Suppression of thymic lymphoma induction by life-long low-dose-rate irradiation accompanied by immune activation in C57BL/6 mice. *Radiat. Res.* **163**, 153–158 (2005).

18. R. E. J. Mitchel, J. S. Jackson and S. M. Carlisle, Upper dose thresholds for radiation-induced adaptive response against cancer in high-dose-exposed, cancer-prone, radiation-sensitive Trp53 heterozygous mice. *Radiat. Res.* **162**, 20–30 (2004).
19. R. E. J. Mitchel, J. S. Jackson, D. P. Morrison and S. M. Carlisle, Low doses of radiation increase the latency of spontaneous lymphomas and spinal osteosarcomas in cancer-prone, radiation-sensitive Trp53 heterozygous mice. *Radiat. Res.* **159**, 320–327 (2003).
20. P. O'Neill and P. Wardman, Radiation chemistry comes before radiation biology. *Int. J. Radiat. Biol.* **85**, 9–25 (2009).
21. C. Grandi and R. Moccaldi, Bystander effect: Critical review and implications for risk assessment in radioprotection. *G. Ital. Med. Lav. Ergon.* **27**, 21–34 (2005).
22. A. I. Kassis, *In vivo* validation of the bystander effect. *Hum. Exp. Toxicol.* **23**, 71 (2004).
23. A. L. Brooks, Evidence for 'bystander effects' *in vivo*. *Hum. Exp. Toxicol.* **23**, 67 (2004).
24. E. I. Azzam and J. B. Little, The radiation-induced bystander effect: evidence and significance. *Hum. Exp. Toxicol.* **23**, 61–65 (2004).
25. Y. Chai and T. K. Hei, Radiation induced bystander effect *in vivo*. *Acta Med. Nagasaki* **53**, 65–69 (2009).
26. B. Djordjevic, Bystander effects: A concept in need of clarification. *BioEssays* **22**, 286–290 (2000).
27. V. P. Bond, V. Benary, C. A. Sondhaus and L. E. Feinendegen, The meaning of linear dose–response relations, made evident by use of absorbed dose to the cell. *Health Phys.* **68**, 786–792 (1995).
28. D. J. Brenner, J. B. Little and R. K. Sachs, The bystander effect in radiation oncogenesis: II. A quantitative model. *Radiat. Res.* **155**, 402–408 (2001).
29. L. E. Feinendegen, The cell dose concept; potential application in radiation protection. *Phys. Med. Biol.* **35**, 597–612 (1990).
30. C. A. Sondhaus, V. P. Bond and L. E. Feinendegen, Cell-oriented alternatives to dose, quality factor, and dose equivalent for low-level radiation. *Health Phys* **59**, 35–48 (1990).
31. ICRP, *1990 Recommendations of the International Commission on Radiological Protection*. Publication 60, *Annals of the ICRP*, Vol. 21, Elsevier, Amsterdam, 1991.
32. M. Matsuoka, F. Nagawa, K. Okazaki, L. Kingsbury, K. Yoshida, U. Muller, D. T. Larue, J. A. Winer and H. Sakano, Detection of somatic DNA recombination in the transgenic mouse brain. *Science* **254**, 81–86 (1991).
33. P. Sykes, A. Hooker, C. Harrington, A. Jacobs, L. Kingsbury and A. Morley, Induction of somatic intrachromosomal recombination inversion events by cyclophosphamide in a transgenic mouse model. *Mutat. Res.* **397**, 209–219 (1998).
34. B. I. Gerashchenko and R. W. Howell, Proliferative response of bystander cells adjacent to cells with incorporated radioactivity. *Cytometry* **60A**, 155–164 (2004).
35. S. M. Goddu, R. W. Howell, L. G. Bouchet, W. E. Bolch and D. V. Rao, *MIRD Cellular S Values: Self-Absorbed Dose Per Unit Cumulate Selected Radionuclides and Monoenergetic Electron and Alpha Emitters Incorportated into Different Cell Compartments*. Society of Nuclear Medicine, Reston, VA, 1997.
36. J. Sheridan and J. Finlay-Jones, Studies of a fractionated murine fibrosarcoma: a reproducible method for the cautious and a caution for the unwary. *J. Cell. Physiol.* **90**, 535–552 (1977).
37. H. Kishikawa, K. Wang, S. J. Adelstein and A. I. Kassis, Inhibitory and stimulatory bystander effects are differentially induced by iodine-125 and iodine-123. *Radiat. Res.* **165**, 688–694 (2006).
38. S. A. Lorimore, J. M. McIlrath, P. J. Coates and E. G. Wright, Chromosomal instability in unirradiated hemopoietic cells resulting from a delayed *in vivo* bystander effect of γ radiation. *Cancer Res.* **65**, 5668–5673 (2005).
39. G. E. Watson, S. A. Lorimore, D. A. Macdonald and E. G. Wright, Chromosomal instability in unirradiated cells induced *in vivo* by a bystander effect of ionizing radiation. *Cancer Res.* **60**, 5608–5611 (2000).
40. L. Y. Xue, N. J. Butler, G. M. Makrigiorgos, S. J. Adelstein and A. I. Kassis, Bystander effect produced by radiolabeled tumor cells *in vivo*. *Proc. Natl. Acad. Sci. USA* **99**, 13765–13770 (2002).
41. M. L. K. Tang, D. A. Steeber, X-Q. Zhang and T. F. Tedder, Intrinsic differences in L-selectin expression levels affect T and B lymphocyte subset-specific recirculation pathways. *J. Immunol.* **160**, 5113–5121 (1998).
42. D. J. Manfra, S. C. Chen, T. Y. Yang, L. Sullivan, M. T. Wiekowski, S. Abbondanzo, G. Vassileva, P. Zalamea, D. N. Cook and S. A. Lira, Leukocytes expressing green fluorescent protein as novel reagents for adoptive cell transfer and bone marrow transplantation studies. *Am. J. Pathol.* **158**, 41–47 (2001).
43. F. Moeller, F. C. Nielsen and L. B. Nielsen, New tools for quantifying and visualizing adoptively transferred cells in recipient mice. *J. Immunol. Methods* **282**, 73–82 (2003).
44. O. Belyakov, M. Folkard, C. Mothersill, K. M. Prise and B. D. Michael, A proliferation-dependent bystander effect in primary porcine and human urothelial explants in response to targeted irradiation. *Br. J. Cancer* **88**, 767–774 (2003).
45. C. Mothersill and C. Seymour, Medium from irradiated human epithelial cells but not human fibroblasts reduces the clonogenic survival of unirradiated cells. *Int. J. Radiat. Biol.* **71**, 421–427 (1997).
46. P. Ren, A. W. de Feijter, D. L. Paul and R. J. Ruch, Enhancement of liver cell gap junction protein expression by glucocorticoids. *Carcinogenesis* **15**, 1807–1813 (1994).
47. S. B. Pruett, N. Obiri and J. L. Kiel, Involvement and relative importance of at least two distinct mechanisms in the effects of 2-mercaptoethanol on murine lymphocytes in culture. *J. Cell. Physiol.* **141**, 40–45 (1989).
48. V. P. Bond, Dose, effect severity, and imparted energy in assessing biological effects. *Stem Cells* **13** (Suppl. 1), 21–29 (1995).
49. V. P. Bond, L. E. Feinendegen and J. Booz, What is a 'low dose' of radiation? *Int. J. Radiat. Biol. Relat. Stud. Phys. Chem. Med.* **53**, 1–12 (1988).
50. Z. Liu, W. V. Prestwich, R. D. Stewart, S. H. Byun, C. E. Mothersill, F. E. McNeill and C. B. Seymour, Effective target size for the induction of bystander effects in medium transfer experiments. *Radiat. Res.* **168**, 627–630 (2007).
51. Z. Liu, C. E. Mothersill, F. E. McNeill, F. M. Lyng, S. H. Byun, C. B. Seymour and W. V. Prestwich, A dose threshold for a medium transfer bystander effect for a human skin cell line. *Radiat. Res.* **166**, 19–23 (2006).
52. L. A. Ryan, R. W. Smith, C. B. Seymour and C. E. Mothersill, Dilution of irradiated cell conditioned medium and the bystander effect. *Radiat. Res.* **169**, 188–196 (2008).
53. E. C. Butcher and W. L. Ford, Following cellular traffic: Methods of labeling lymphocytes and other cells to trace their migration *in vivo*. In *Handbook of Experimental Immunology: Cellular Immunology* (D. Weir, Ed.), pp. 1–23. Blackwell Scientific, Oxford, 1986.
54. J. W. Albright, R. C. Mease, C. Lambert and J. F. Albright, Effects of aging on the dynamics of lymphocyte organ distribution in mice: use of a radioiodinated cell membrane probe. *Mech. Ageing Dev.* **101**, 197–211 (1998).
55. S. Elmore, Enhanced histopathology of the spleen. *Toxicol. Pathol.* **34**, 648–655 (2006).
56. F. M. Lyng, P. Maguire, B. McClean, C. Seymour and C. Mothersill, The involvement of calcium and MAP kinase signaling pathways in the production of radiation-induced bystander effects. *Radiat. Res.* **165**, 400–409 (2006).
57. F. M. Lyng, C. B. Seymour and C. Mothersill, Production of a signal by irradiated cells which leads to a response in unirradiated cells characteristic of initiation of apoptosis. *Br. J. Cancer* **83**, 1223–1230 (2000).

58. C. Mothersill, R. J. Seymour and C. B. Seymour, Increased radiosensitivity in cells of two human cell lines treated with bystander medium from irradiated repair-deficient cells. *Radiat. Res.* **165**, 26–34 (2006).

59. O. A. Sedelnikova, A. Nakamura, O. Kovalchuk, I. Koturbash, S. A. Mitchell, S. A. Marino, D. J. Brenner and W. M. Bonner, DNA double-strand breaks form in bystander cells after microbeam irradiation of three-dimensional human tissue models. *Cancer Res.* **67**, 4295–4302 (2007).

60. H. Aviles, M. Johnson and F. Monroy, Effects of cold stress on spleen cell proliferation and cytokine production during chronic *Toxoplasma gondii infection. Neuroimmunomodulation* **11**, 93–102 (2004).

61. K. Cho, L. Adamson, J. Park and D. Greenhalgh, Burn injury-mediated alterations in cell cycle progression in lymphoid organs of mice. *Shock* **19**, 138–143 (2003).

62. S. Fan, S. Gao, L. Shao, Y. Li, L. Mei and G. Ding, A factor in lymph node and spleen induced by restraint stress in mice and rats suppresses lymphocyte proliferation. *Neuroimmunomodulation* **2**, 274–281 (1995).

63. I. Kovshik, A. Silkov, S. Sennikov, A. Shurlygina and V. Trufakin, Proliferative activity of cells in mouse thymus and spleen under different diurnal regimens of interleukin-2 administration. *Bull. Exp. Biol. Med.* **142**, 98–101 (2006).

64. Y. Sakaguchi, L. C. Stephens, M. Makino, T. Kaneko, F. R. Strebel, L. L. Danhauser, G. N. Jenkins and J. M. C. Bull, Apoptosis in tumors and normal tissues induced by whole body hyperthermia in rats. *Cancer Res.* **55**, 5459–5464 (1995).

65. J. Wang, R. Charboneau, R. A. Barke, H. H. Loh and S. Roy, Mu-opioid receptor mediates chronic restraint stress-induced lymphocyte apoptosis. *J. Immunol.* **169**, 3630–3636 (2002).

66. L. X. Wei, J. N. Zhou, A. I. Roberts and Y. F. Shi, Lymphocyte reduction induced by hindlimb unloading: distinct mechanisms in the spleen and thymus. *Cell Res.* **13**, 465–471 (2003).

67. D. Yin, D. Tuthill, R. A. Mufson and Y. Shi, Chronic restraint stress promotes lymphocyte apoptosis by modulating CD95 expression. *J. Exp. Med.* **191**, 1423–1428 (2000).

68. G. Schettino, M. Folkard, B. D. Michael and K. M. Prise, Low-dose binary behavior of bystander cell killing after microbeam irradiation of a single cell with focused C_K X rays. *Radiat. Res.* **163**, 332–336 (2005).

69. S. Z. Liu, S. Z. Jin and X. D. Liu, Radiation-induced bystander effect in immune response. *Biomed. Environ. Sci.* **17**, 40–46 (2004).

70. B. I. Gerashchenko and R. W. Howell, Cell proximity is a prerequisite for the proliferative response of bystander cells co-cultured with cells irradiated with gamma-rays. *Cytometry A* **56**, 71–80 (2003).

71. M. Boyd, S. C. Ross, J. Dorrens, N. E. Fullerton, K. W. Tan, M. R. Zalutsky and R. J. Mairs, Radiation-induced biologic bystander effect elicited in vitro by targeted radiopharmaceuticals labeled with α-, β-, and Auger electron-emitting radionuclides. *J. Nucl. Med.* **47**, 1007–1015 (2006).

72. R. Persaud, H. Zhou, T. K. Hei and E. J. Hall, Demonstration of a radiation-induced bystander effect for low dose low LET beta-particles. *Radiat. Environ. Biophys.* **46**, 395–400 (2007).

73. C. Mothersill, F. Lyng, C. Seymour, P. Maguire, S. Lorimore and E. Wright, Genetic factors influencing bystander signaling in murine bladder epithelium after low-dose irradiation *in vivo*. *Radiat. Res.* **163**, 391–399 (2005).

74. S. A. Lorimore, J. A. Chrystal, J. I. Robinson, P. J. Coates and E. G. Wright, Chromosomal instability in unirradiated hemaopoietic cells induced by macrophages exposed *in vivo* to ionizing radiation. *Cancer Res.* **68**, 8122–8126 (2008).

75. C. Mothersill, D. Rea, E. G. Wright, S. A. Lorimore, D. Murphy, C. B. Seymour and K. O'Malley, Individual variation in the production of a 'bystander signal' following irradiation of primary cultures of normal human urothelium. *Carcinogenesis* **22**, 1465–1471 (2001).

76. A. Acheva, R. Georgieva, I. Rupova, R. Boteva and F. Lyng, Bystander responses in low dose irradiated cells treated with plasma from gamma irradiated blood. *J. Phys. Conf. Ser.* **101**, 012005 (2008).